Cancer Cell
Article

Directed Phenotype Switching as an Effective Antimelanoma Strategy

Magalí Sáez-Ayala,[1,6] María F. Montenegro,[1,6] Luis Sánchez-del-Campo,[2,6] María Piedad Fernández-Pérez,[1] Soledad Chazarra,[1] Rasmus Freter,[2] Mark Middleton,[3] Antonio Piñero-Madrona,[4] Juan Cabezas-Herrera,[5] Colin R. Goding,[2,*] and José Neptuno Rodríguez-López[1,*]

[1]Department of Biochemistry and Molecular Biology A, School of Biology, Regional Campus of International Excellence "Campus Mare Nostrum", University of Murcia, 30100 Murcia, Spain
[2]Nuffield Department of Clinical Medicine, Ludwig Institute for Cancer Research, University of Oxford, Headington, Oxford OX3 7DQ, UK
[3]Department of Oncology, Oxford NIHR Biomedical Research Centre, Churchill Hospital, Oxford OX3 7LE, UK
[4]Department of Surgery
[5]Translational Cancer Research Group
University Hospital Virgen de la Arrixaca, Instituto Murciano de Investigación Biosanitaria, 30120 Murcia, Spain
[6]These authors contributed equally to this work
*Correspondence: colin.goding@ludwig.ox.ac.uk (C.R.G.), neptuno@um.es (J.N.R.-L.)
http://dx.doi.org/10.1016/j.ccr.2013.05.009

SUMMARY

Therapeutic resistance in melanoma and other cancers arises via irreversible genetic, and dynamic phenotypic, heterogeneity. Here, we use directed phenotype switching in melanoma to sensitize melanoma cells to lineage-specific therapy. We show that methotrexate (MTX) induces microphthalmia-associated transcription factor (MITF) expression to inhibit invasiveness and promote differentiation-associated expression of the melanocyte-specific *Tyrosinase* gene. Consequently, MTX sensitizes melanomas to a tyrosinase-processed antifolate prodrug 3-*O*-(3,4,5-trimethoxybenzoyl)-(−)-epicatechin (TMECG), that inhibits the essential enzyme DHFR with high affinity. The combination of MTX and TMECG leads to depletion of thymidine pools, double-strand DNA breaks, and highly efficient E2F1-mediated apoptosis in culture and in vivo. Importantly, this drug combination delivers an effective and tissue-restricted antimelanoma therapy in vitro and in vivo irrespective of *BRAF*, *MEK*, or p53 status.

INTRODUCTION

Cancer initiation arises via the stepwise acquisition of mutations that suppress senescence and promote cell division to lead to tumor formation. Subsequently, cells within the primary tumor may acquire properties of invasiveness and metastasize to seed new tumors. Despite several decades of research, almost half of patients diagnosed with cancer die of the disease, primarily because of metastases, and surgery remains the most effective therapy. The failure of current approaches to cancer therapy reflects an underlying problem that has long been recognized (Fidler, 1978), but which is only beginning to be understood at the molecular level: cancer cell population heterogeneity. Irreversible accumulation of genetic lesions may give rise to cell populations with a capacity to bypass therapies targeted specifically toward key molecules. Superimposed on genetic variation is reversible heterogeneity dictated by microenvironmental signaling; within tumors, multiple subpopulations of cancer cells may coexist, each with differing biological properties. Some may exhibit features of differentiation, others proliferate, whereas some may possess stem cell-like properties (Brabletz et al., 2005; Visvader and Lindeman, 2008), able to initiate new tumors and provide a pool of therapeutically resistant cells (Blagosklonny, 2005). For therapies to be effective, two key criteria should be fulfilled: the therapy should be effective independent of the driver mutations within the cancer, so as to avoid resistance arising from genetic

Significance

There is currently no effective long-term treatment for metastatic melanoma; resistance to the recently developed BRAF inhibitors occurs within some months, and there is no effective therapy for BRAF-negative melanomas where resistance to chemotherapy may arise from the presence of invasive slow-cycling melanoma stem-like cells. By contrast, the two-step strategy applied here uses methotrexate, a drug already in widespread clinical use, to direct melanoma cells away from an invasive state, and then targets an essential enzyme in a melanoma-specific fashion to induce highly efficient apoptosis. As a result, we describe a potent antimelanoma therapy that is highly effective in preclinical trials irrespective of *BRAF* or p53 status and validate the concept of directed phenotype switching as a therapeutic option.

diversity within signaling pathways, and potentially resistant phenotypic subpopulations should be directed toward a sensitive phenotype. Understanding the origins of cancer cell heterogeneity and how it can be managed to provide more effective treatments is therefore a key issue.

Melanoma, a highly aggressive skin cancer with very poor prognosis for metastatic disease, is driven by mutations that activate mitogen-activated protein kinase (MAPK) signaling, combined with senescence bypass (Bennett, 2008; Lopez-Bergami, 2011). Around 50% of melanomas bear activating mutations in *BRAF* (Davies et al., 2002), whereas a further 15%–20% express activated NRAS (van Elsas et al., 1995), and a lower proportion activation of MEK (Nikolaev et al., 2012), or other factors that activate MAPK signaling such as Kit (Curtin et al., 2006) or GNAQ (Van Raamsdonk et al., 2009). Consistent with genetic heterogeneity playing a major role in therapeutic resistance, targeting activated BRAF with vemurafenib leads to dramatic and rapid tumor regression that relapses after some months (Sosman et al., 2012; Villanueva et al., 2011), with resistance arising from activating mutations in other factors that bypass the requirement for activated BRAF in MAPK signaling (Fedorenko et al., 2011; Nazarian et al., 2010). Although combining BRAF inhibition with molecules that target other components of the MAPK pathway is currently being investigated (Smalley and Flaherty, 2009), it is clear that even for targeted therapies, genetic heterogeneity represents a major challenge to effective therapy. An alternative strategy, that would bypass the genetic resistance arising from targeting specific components of the MAPK pathway, would be to identify compounds that act on all melanomas irrespective of how MAPK signaling is activated.

Advances in understanding the genetics underpinning melanoma progression have been complemented by observations that the microphthalmia-associated transcription factor (MITF) (Arnheiter, 2010; Hodgkinson et al., 1993) acts as a rheostat in determining subpopulation identity (Carreira et al., 2006; Cheli et al., 2012; Hoek and Goding, 2010). In melanomas, reduced MITF expression leads to G1 arrested, invasive cells with stem-like properties (Carreira et al., 2006; Cheli et al., 2011), including the ability to initiate tumors with high efficiency. Low levels of MITF, driven by transcriptional repression by the BRN-2 (POU3f2) transcription factor (Goodall et al., 2008; Kobi et al., 2010), lead to a p27-mediated cell-cycle arrest and an invasive stem cell-like phenotype (Carreira et al., 2006; Cheli et al., 2011; Pinner et al., 2009). By contrast, elevated MITF leads to activation of differentiation genes driving melanin production such as *TYROSINASE* (*TYR*) and melanosome biogenesis (Carreira et al., 2005; Cheli et al., 2010; Loercher et al., 2005). Consequently, tumors comprise a mix of MITF-positive and negative melanoma cells (Goodall et al., 2008). As such, modulation of MITF expression represents one approach toward driving heterogeneous populations of tumor cells to a therapeutically sensitive phenotype.

Although MITF is required for melanoma proliferation (Carreira et al., 2006), and has been described as a lineage addiction oncogene, decreasing MITF expression as proposed (Garraway et al., 2005) would potentially lead to an increase in invasive melanoma cells (Carreira et al., 2006; Cheli et al., 2011). Here, we take the opposite approach to therapy and screen for molecules that upregulate MITF, with the aim of eradicating invasive melanoma cells and at the same time sensitizing cells to a TYR-processed antifolate prodrug 3-*O*-(3,4,5-trimethoxybenzoyl)-(−)-epicatechin (TMECG).

RESULTS

Methotrexate Stimulates MITF Expression to Induce Differentiation in Melanoma Cells

MITF's role in determining melanoma cell phenotype suggested a two-step therapeutic approach (Figure 1A) that would circumvent many problems associated with both genetic and phenotypic heterogeneity. First is to elevate MITF expression to eradicate invasive cells and then to use the MITF-induced melanocyte-specific enzyme TYR to activate a prodrug able to target an enzyme critical to cell viability in a cell-type-specific fashion. We therefore screened for molecules that elevate MITF levels and identified methotrexate (MTX), a differentiating agent and slow-tight binding competitive inhibitor of dihydrofolate reductase (DHFR) in widespread clinical use, as an effective activator of MITF expression. After treating melanoma cells with MTX, the level of *MITF* messenger (mRNA) was increased compared to untreated controls in three melanoma cell lines (Figure 1B). MITF protein levels were also upregulated in human (SK-MEL-28, G361, A375) and murine (B16/F10) MTX-treated melanoma cells as shown by western blot (Figure 1C), and by confocal microscopy analyses in 501 MEL cells (Figure 1D). Importantly MTX also upregulated MITF expression in the amelanotic and highly invasive melanoma cell line IGR39 (Figure 1C, lower panel), and consistent with our predictions, MTX-mediated upregulation of MITF prevented invasiveness of both SK-MEL-28 and IGR39 cells in a matrigel Boyden chamber assay (Figure 1E). The reduction in invasiveness on MTX addition was mediated by increased MITF expression, because small-interfering-RNA (siRNA)-mediated depletion of MITF reversed the effect of MTX (Figure S1 available online).

To determine whether MTX-induced changes in MITF levels were accompanied by an increase in the transcriptional activity of MITF, we performed chromatin immunoprecipitation (ChIP) assays to determine the occupancy of this transcription factor on the promoters of the *PMEL17* and *TYR* genes, both well-characterized MITF targets (Cheli et al., 2010; Du et al., 2003) (Figure 2A). Compared with untreated SK-MEL-28 cells, MTX substantially increased the occupancy of MITF on the *TYR* promoter (from 1.5% in untreated cells to 25.2% in MTX-treated cells with respect to an input control) and on the promoter/enhancer of the *Pmel17* gene (from 5.4% in untreated cells to 45.4% in MTX-treated cells with respect to an input control). No binding was observed to control regions lacking MITF target sites.

Using scanning electron microscopy (Figure 2B), we observed that a single treatment with MTX strongly stimulated melanoma cell dendricity, a morphological feature of differentiated melanocytes controlled by MITF (Carreira et al., 2005; Tachibana et al., 1996) and the first observable parameter of melanoma cell differentiation (Serafino et al., 2004). Consistent with these data, quantitative real-time RT-PCR (Figure 2C) revealed that MTX increased mRNA expression of the MITF differentiation targets *TYR*, *PMEL17*, *RAB27a*, *TYRP1*, and *MART1* (Cheli et al., 2010) that was prevented by MITF-specific siRNA. The increased mRNA expression of MITF targets was matched by

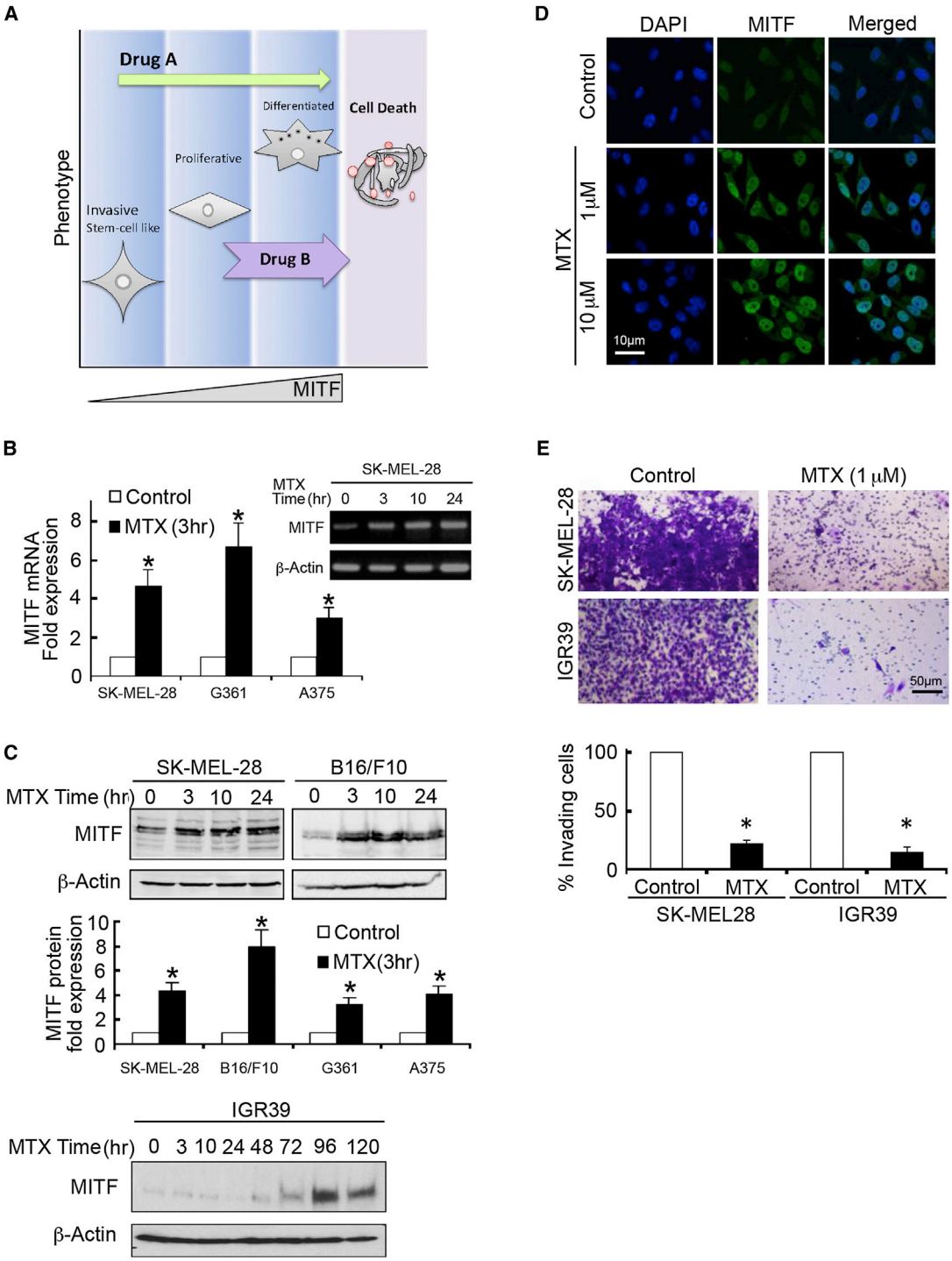

Figure 1. MTX Upregulates the Expression of MITF and Blocks Invasiveness

(A) The MITF rheostat and the two-step strategy for melanoma therapy. Drug A induces MITF, eliminating invasive cells and driving cells to be sensitive to drug B.

(B) MTX (1 μM) increases *MITF* mRNA determined using quantitative and conventional RT-PCR from indicated cell lines. Asterisks denote statistically significant differences ($p < 0.05$).

(C) MTX (1 μM) induces MITF protein assayed by western blotting (*WB*) (*$p < 0.05$).

(D) Immunofluorescence of control or MTX-treated (3 hr) 501 MEL cells using anti-MITF and DAPI. Scale bar refers to all panels.

(E) Matrigel assay of control and MTX-treated SK-MEL-28 (48 hr, 1 μM) and IGR39 (72 hr, 1 μM) cells. Asterisks denote statistically significant differences (*$p < 0.05$). Scale bar refers to all panels.

Error bars in the entire figure show mean ± SD.

See also Figure S1.

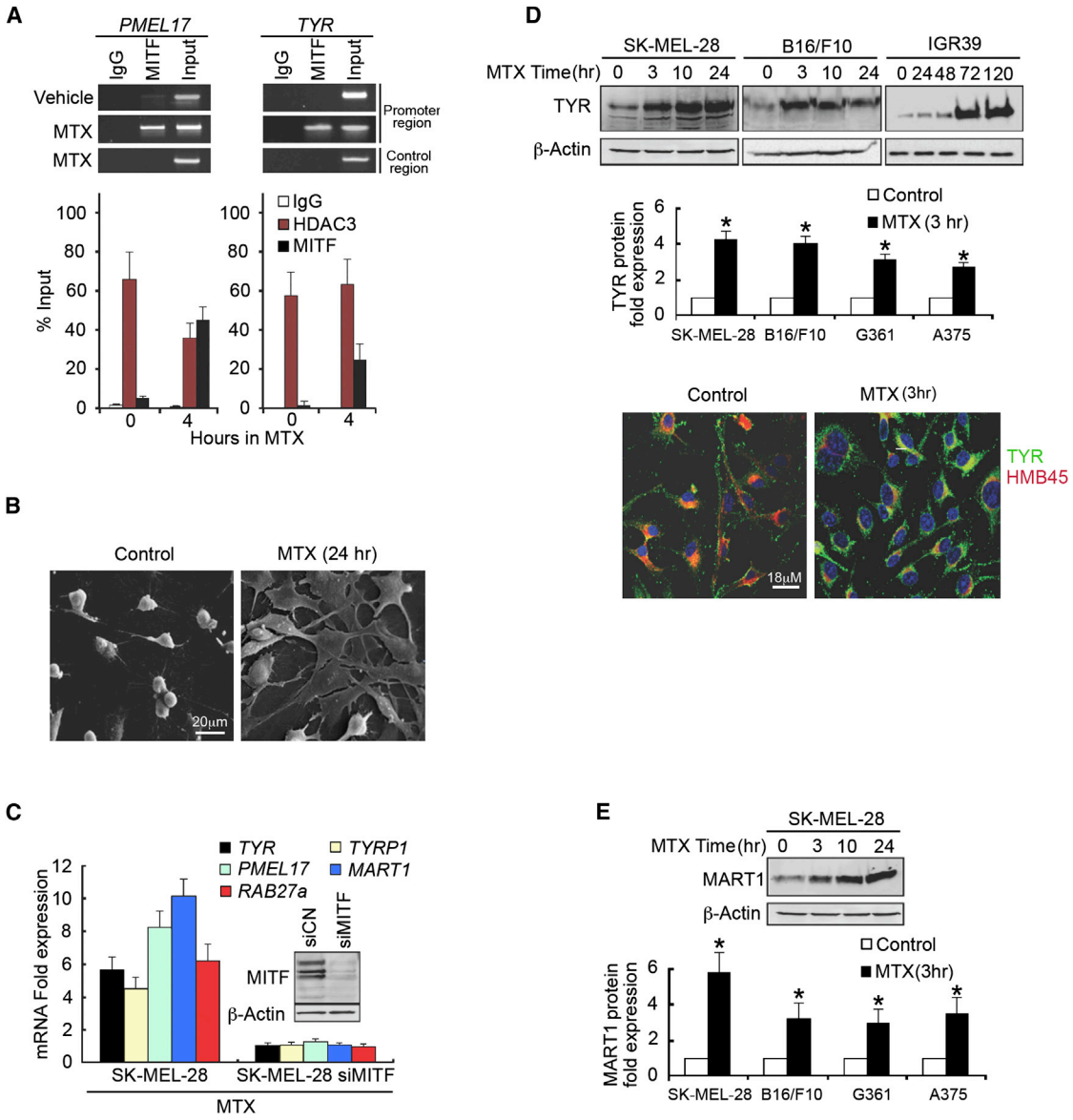

Figure 2. MTX Promotes Melanoma Differentiation

(A) Chromatin immunoprecipitation on *TYR* and *Pmel17* genes of vehicle and MTX-treated (4 hr, 1 μM) SK-MEL-28 with semiquantitative PCR after immunoprecipitation (upper panel) or quantitative real-time PCR (graphs) with IgG, or MITF and HDAC3 antibodies. Error bars indicate SDs of triplicates; experiment reproduced four times with similar results. Primers were used to amplify the promoter and control regions of *TYR* and *PMEL17* genes.

(B) Scanning electron micrographs of control and MTX-treated (1 μM, 24 hr) SK-MEL-28 cells. Scale bar is applicable to both panels.

(C) Quantitative RT-PCR of *TYR*, *TYRP1*, *PMEL17*, *MART1*, and *RAB27a* mRNA. SK-MEL-28 and siMITF-SK-MEL-28 cells were treated for 5 hr with 1 μM MTX. mRNA levels are presented relative to β-actin mRNA and compared to their expression levels in untreated cells (1-fold). Induction of all genes by MTX was statistically significant ($p < 0.05$), except in siMITF-SK-MEL-28 cells. *WB* indicates efficiency of MITF knockdown using *MITF*-specific stealth RNA oligonucleotide (siMITF) compared to control (siCN).

(D) *WB* for TYR in indicated cell lines (upper panels) following MTX treatment for indicated times; and immunofluorescence for TYR (green) and the melanosome stage II marker, HMB45 (red) (lower panels), in SK-MEL-28 cells before (control) and after MTX (1 μM 3 hr) treatment. DAPI is represented in blue. Scale bar is applicable to both panels.

(E) *WB* of MART1 protein levels in melanoma cell lines (*$p < 0.05$) following MTX treatment (1 μM).

Error bars in the entire figure show mean ± SD.

upregulation of TYR protein expression in multiple melanoma cell lines, including the amelanotic cell line IGR39, as detected by either western blot or immunofluorescence (Figure 2D) and MART1 (Figure 2E).

MTX-Induced MITF Expression Renders Melanomas Sensitive to Prodrug Therapy

The increased *TYR* expression in response to MTX-mediated MITF activation provided an opportunity to implement the

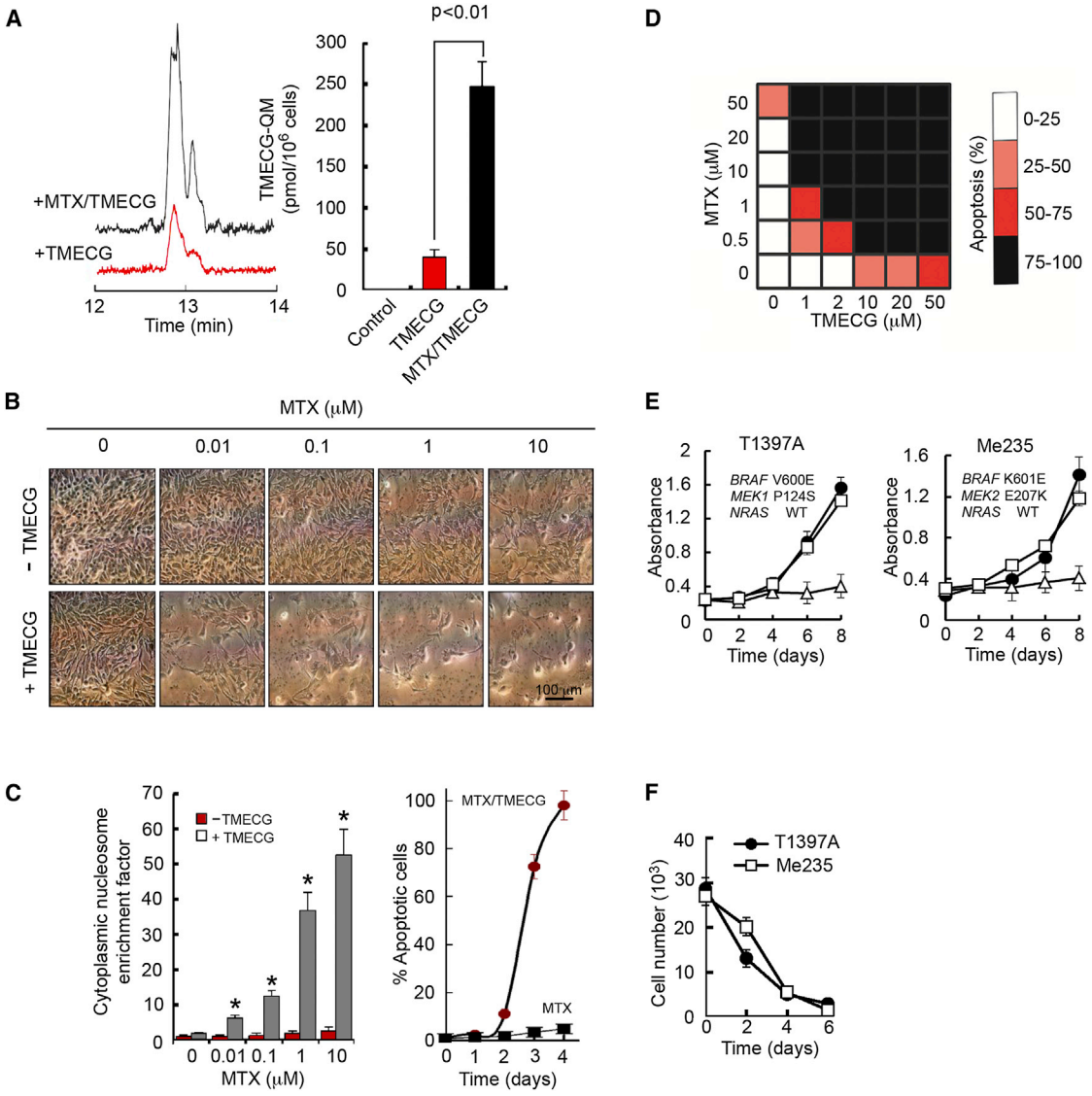

Figure 3. A Combined Treatment with MTX and TMECG Inhibits Melanoma Growth and Induces Apoptosis in Cultures of Human Cells

(A) The intracellular accumulation of TMECG-QM species in SK-MEL-28 cells after 24 hr of treatment with 10 μM TMECG or 1 μM MTX plus 10 μM TMECG. The left panel shows the HPLC-MS chromatograms.

(B) Proliferation assays performed using SK-MEL-28 of control cells or cells treated with indicated doses of MTX with or without 10 μM TMECG. Scale bar = 100 μm and refers to all panels.

(C) Quantification of effects of MTX/TMECG treatment on SK-MEL-28 cells (*$p < 0.05$ with respect to TMECG-treated cells [TMECG] = 10 μM). For time course assay MTX (1 μM) and TMECG (10 μM) were used.

(D) Apoptosis determination at different MTX/TMECG combinations in SK-MEL-28 cells after 4 days of treatment. Data were obtained in triplicate in two independent experiments. Differences in apoptosis in MTX/TMECG-treated cells were significant with respect to individual treatments for each drug concentration ($p < 0.05$).

(E) MTT assay indicating effects of MTX/TMECG (1 μM/10 μM) and PLX-4720 (1 μM) treatment on low passage patient-derived melanoma cells bearing indicated *MEK* and *BRAF* mutations. Cells were treated with vehicle only (●), PLX-4720 (□), or with a combination of MTX + TMECG (△). Note the number of cells at the start of the experiment was at the limit of detection.

(F) Effects of MTX/TMECG (1 μM/10 μM) on cell number of indicated cell lines.

Error bars show mean ± SD.

See also Figure S2 and Table S1.

second arm of the two-step strategy (Figure 1A). TMECG is an antifolate prodrug (Sánchez-del-Campo et al., 2009a) we designed to be activated by TYR, in effect generating a cell-type-specific cytotoxic agent. HPLC-MS/MS experiments confirmed that MTX-induced TYR overexpression greatly contributed to the activation of the prodrug TMECG to its corresponding quinone methide (TMECG-QM) (Figure 3A; Table S1) that acts as a potent and irreversible competitive inhibitor of DHFR for

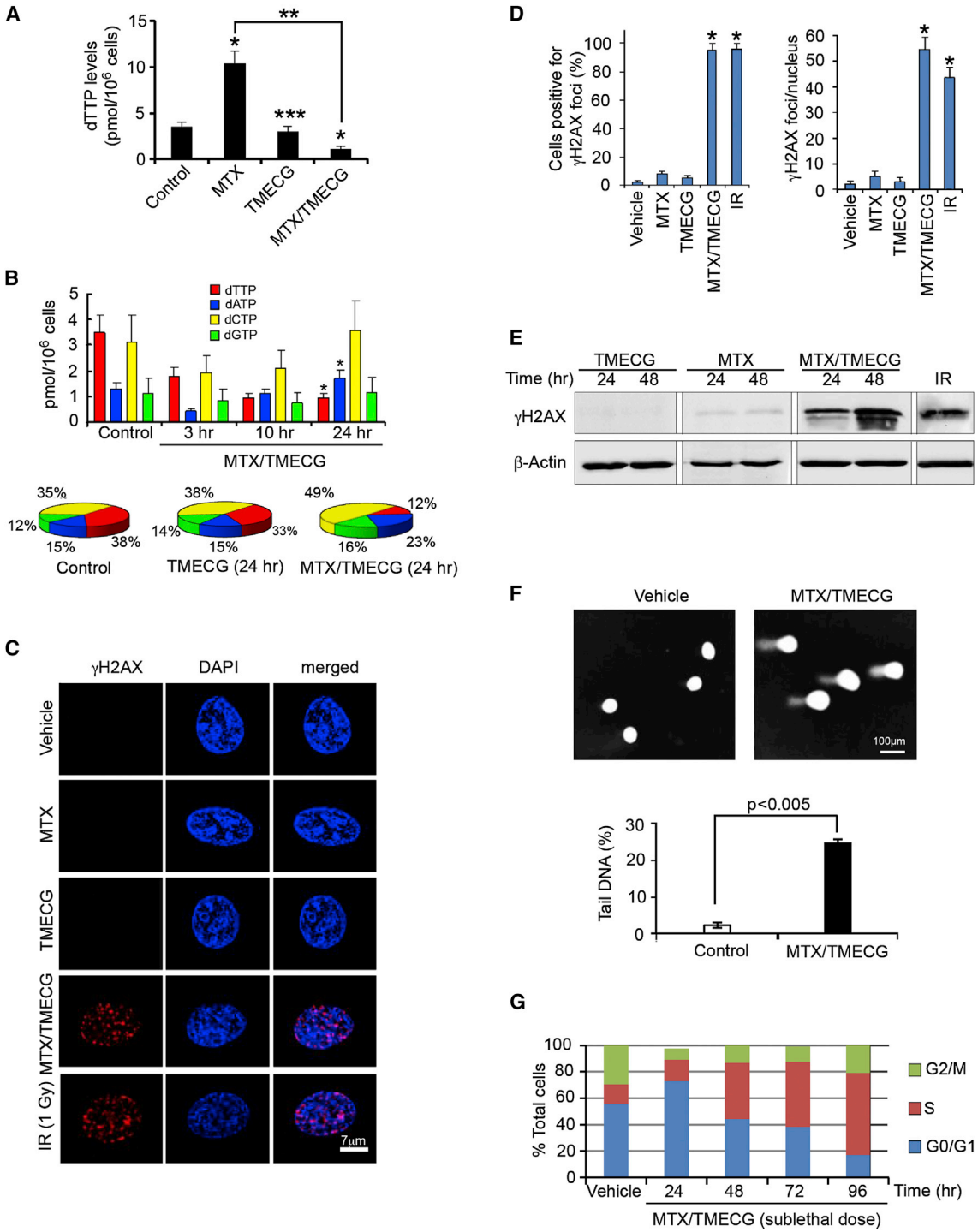

Figure 4. MTX and TMECG Combination Therapy Induces Apoptosis via dTTP Depletion and DNA Damage

(A) dTTP quantification in melanoma cells subjected to indicated treatments. *p < 0.05 with respect to untreated controls; **p = 0.001; ***Not statistically significant with respect to the untreated controls.

(B) Quantification of all dNTPs in melanoma cells treated with MTX/TMECG (1 μM/10 μM).

(C) SK-MEL-28 cells treated with MTX (1 μM) and/or TMECG (10 μM), or X-rays (1 Gy) were examined by immunofluorescence for γH2AX foci (red) and DAPI (blue). Scale bar = 7 μm and refers to all panels.

(D) Quantification of γH2AX foci in SK-MEL-28 cells treated with MTX (1 μM) and/or TMECG (10 μM), or X-rays. Histograms represent the positive γH2AX foci cells and γH2AX foci/nucleus in positive γH2AX foci cells (*p < 0.01 when compared with untreated cells or those subjected to MTX and TMECG individuals treatments).

(E) Detection of γH2AX by *WB* in SK-MEL-28 cells treated with MTX and/or TMECG. β-actin served as a protein loading control.

(legend continued on next page)

dihydrofolate (DHF) (Sánchez-del-Campo et al., 2009a). Treatment of SK-MEL-28 cells with MTX alone reduced proliferation but did not induce apoptosis, (Figure 3B, upper panels), consistent with elevated MITF levels leading to reduced proliferation (Carreira et al., 2005). By contrast, MTX at concentrations as low as 10 nM in combination with TMECG led to substantial apoptosis (Figure 3B, lower panels) and induced MITF expression (Figure S2A). The combination of a single dose of MTX and TMECG was also highly effective, with apoptosis occurring in close to 100% of cells after 4 days treatment (Figure 3C), and titration of both compounds demonstrated they acted synergistically (Figure 3D). Importantly, MTX/TMECG targeted melanoma cell lines independently of the mutational status of genes such as *p53 (TP53) BRAF*, *NRAS*, or *PTEN* and was also effective in the amelanotic melanoma cell line IGR39 (Figure S2B). This raised the possibility that MTX/TMECG would also be effective against BRAF mutant melanomas that have developed genetic resistance to BRAF and/or MEK inhibitors. We therefore tested the effectiveness of MTX/TMECG on two low passage melanoma cell lines (fewer than 10 passages) derived from patients with activating BRAF mutations that are resistant to both BRAF-inhibitor and MEK-inhibitor therapy because they also have activating mutations in *MEK1* or *MEK2* (Nikolaev et al., 2012). In these MTT assays (Figures 3E and S2B), we used a low starting number of cells (2×10^3) so that any proliferation could be readily visualized. As expected, the PLX-4720 inhibitor of activated BRAF failed to impact significantly on proliferation (Figure 3E). By contrast, the MTX/TMECG combination therapy was highly effective. By starting with 3×10^4 cells and counting cell numbers, the effectiveness of MTX/TMECG in inducing cell death in these drug-resistant cells was readily apparent (Figure 3F). Similar effects were seen on melanoma cells derived from dissociated fresh melanoma metastases isolated directly from patients (Figure S2C). To distinguish between melanoma and nonmelanoma cells in the freshly dissociated tumors, we used a *DOPACHROME TAUTOMERASE* (*DCT*) promoter-mCherry reporter virus that expresses mCherry only in the melanocyte lineage. In this case, MTX/TMECG treatment for 6 days led to a 5-fold reduction in mCherry-positive cells indicating effectiveness in cells directly isolated from patient-derived tissue.

To verify that MTX/TMECG synergy is cell type specific, we also performed titration experiments in melanoma (SK-MEL-28, G361), breast (MCF7), and colon (Caco-2) cancer cell lines (Figure S2D). As expected the melanoma cell lines were substantially less sensitive to MTX alone than the nonmelanoma lines. The sensitivity to TMECG alone was between 2- and 5-fold greater in the melanoma cell lines because both melanoma cell lines express low levels of TYR. However, MTX synergistically increased the sensitivity of the melanoma cells to TMECG, presumably by upregulating MITF and TYR, whereas in the nonmelanoma cell lines the effects were at best additive. siRNA-mediated depletion of MITF (Figure S2E), or TYR (Figure S2F), substantially reduced cell death and confirmed their key requirement for the effectiveness of the MTX/TMECG drug combination. Thus, the synergy between the two compounds appears limited to TYR-positive melanoma cells, a key aim in the design of a cell-type-specific antimelanoma therapy.

MTX/TMECG Combination Therapy Promotes dTTP Depletion and DNA Damage

The results so far indicate that, counterintuitively, two different drugs that both target DHFR, synergistically kill melanoma cells. DHFR is required for dTTP synthesis, and in most cancer cells its inhibition by MTX leads to decreased dTTP levels (Wang et al., 2005). By contrast in melanoma, MTX alone leads to increased dTTP levels, whereas dTTP was significantly reduced by the MTX/TMECG combination (Figure 4A), leading to a nucleotide imbalance (Figure 4B). The ability of MTX to elevate dTTP in melanoma, but not other cancer types may be partly explained by the fact that *DHFR* is regulated by MITF (Strub et al., 2011; data not shown), which is strongly upregulated by MTX. Moreover, because TMECG-QM acts as a competitive inhibitor of DHFR with respect to DHF, the observed MTX-dependent depletion of this substrate (Table S1) could explain the high synergy observed upon cotreatment with MTX and TMECG in melanoma cells (Figures 3, S2B, and S2D) where TYR converts TMECG to its quinone methide (Figure 3A).

Thymidine depletion induces DNA double-strand break (DSB) formation (Pardee et al., 2004) characterized by phosphorylation of histone H2AX at Ser^{139} (γH2AX) by ATM/ATR kinases and the subsequent rapid formation of γH2AX foci at the DSB sites (Kinner et al., 2008). Consistent with the effects of combination treatment being mediated via thymidine depletion, immunofluorescence revealed that combined MTX/TMECG treatment of SK-MEL-28 cells, but not MTX or TMECG alone, led to accumulation of γH2AX foci by 48 hr (Figures 4C and 4D), a result confirmed by western blotting (Figure 4E). The increase in γH2AX foci was accompanied by the induction of DSBs as determined using a comet assay (Figure 4F). Moreover, consistent with the MTX/TMECG combination causing S phase-associated DNA damage, sublethal doses of MTX/TMECG coupled with flow cytometry revealed accumulation of cells in S phase (Figure 4G).

MTX/TMECG Combination Therapy Induces E2F1-Mediated Apoptosis in Melanoma Cells

p53 is usually wild-type (WT) in melanoma (Box and Terzian, 2008). However, apoptosis triggered by MTX/TMECG was independent of p53 mutation status (Figures 5A and S2B). Consistent with this, although p53 protein levels were upregulated by MTX/TMECG, presumably as a consequence of DNA damage (Figure S3A), apoptosis was unaffected by p53 silencing (Figure 5A). Although p53 mRNA levels in SK-MEL-28 cells did not change in the presence of MTX/TMECG (Figure 5B), MTX and TMECG combined dramatically induced the mRNA (Figure 5B) and protein expression (Figure 5B, lower panels) of the apoptosis protease-activating factor 1 (APAF1), as well as the mRNA (Figure 5B) and protein (Figure 5C, lower panels) of the proapoptotic transactivating form of p73 (TAp73).

(F) Comet assay of SK-MEL-28 treated with vehicle or MTX/TMECG (1 μM/10 μM) for 48 hr. Hydrogen peroxide was used as a positive control (data not shown). Scale bar refers to both panels.
(G) Cell-cycle profile determined by flow cytometry of SK-MEL-28 cells treated with a sublethal dose of MTX/TMECG.
Error bars show mean ± SD.

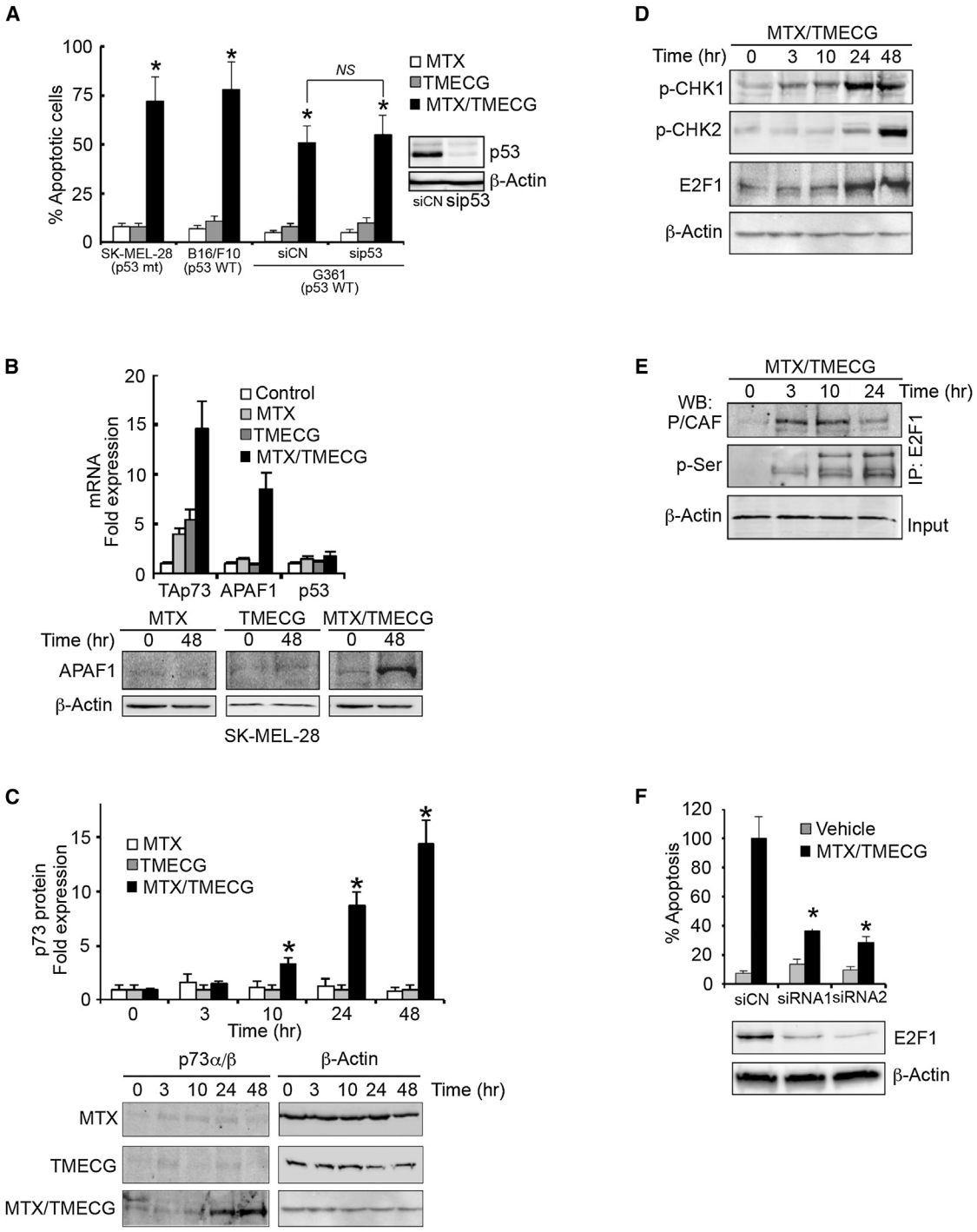

Figure 5. MTX/TMECG Treatment Induces E2F1 and p73

MTX (1 μM) and TMECG (10 μM) were used (for all changes *p < 0.05 with respect to individual treatments in all experiments). Error bars show mean ± SD.

(A) Indicated combinations of drugs were added to melanoma cell lines (p53 status indicated) and apoptosis determined after 3 days. p53 was silenced in G361 cells as indicated and shown in inset *WB*.

(B) Quantitative RT-PCR analysis of TAp73, p53, and Apaf1 (upper panel) in SK-MEL-28 treated with MTX and/or TMECG. Apaf1 protein levels are shown (lower panel). β-actin was used as a protein loading control. mRNA levels are presented relative to β-actin mRNA.

(C) p73 protein levels were evaluated by *WB* over time following indicated treatments. β-actin expression indicated that an equal amount of protein was loaded for each sample.

(D) *WB* of p-Chk1, p-Chk2, and E2F1 after MTX/TMECG treatment.

(E) Immunoprecipitation of E2F1 from control or MTX/TMECG-treated SK-MEL-28 cells *WB* of immunoprecipitates using indicated antibodies. β-actin served as a protein loading control.

(legend continued on next page)

p73 (*TP73*) expression is controlled by E2F1 (Dobbelstein et al., 2005), which, in turn, is stabilized by phosphorylation by Chk2 at Ser^{364}, ATM kinase at Ser^{31}, or acetylation by P/CAF at lysines 117, 120, and 125 (Lin et al., 2001; Martínez-Balbás et al., 2000; Urist et al., 2004) (Figure S3B). DNA damage induced by the MTX/TMECG combination led to a time-dependent increase in Chk1 and Chk2 phosphorylation and increased E2F1 protein (Figure 5D). Consistent with this, immunoprecipitation of E2F1 revealed that MTX/TMECG increased its phosphorylation and association with the P/CAF acetyl transferase (Figure 5E).

Mass spectrometry analysis of immunoprecipitated E2F1 confirmed that MTX/TMECG increased both phosphorylation (Figure S3C) and acetylation of E2F1, and also revealed loss of methylation of E2F1 at Lys^{185} (Table S2) (Kontaki and Talianidis, 2010), a modification that inhibits acetylation, promotes E2F1-degradation, and prevents stabilization of E2F1 in response to DNA damage (Hallstrom et al., 2008). siRNA-mediated silencing of E2F1 (Figure 5F) significantly decreased the sensitivity of SK-MEL-28 cells to MTX/TMECG-induced apoptosis compared to a control siRNA (siCN). Although we cannot rule out that E2F1 depletion blocks apoptosis by preventing passage to S phase, collectively the data are consistent with a mechanism by which manipulating MITF, and consequently TYR levels, via MTX treatment renders melanoma cells sensitive to TMECG-induced depletion of dTTP pools and p53-independent and E2F1-driven apoptosis.

MTX/TMECG Is Highly Effective In Vivo

The profound effects of the MTX/TMECG combination in vitro led us to test its antitumorigenic efficacy in vivo. First, we used a reconstituted skin model of melanoma in which melanocytes were replaced by A375 melanoma cells (Figure 6A). Twenty-one days following tumor cell implantation, massive melanoma nodes were observed within the epidermis, and evidence of early metastasis into dermal structures was observed in untreated skin. Both MTX and TMECG alone reduced, but did not abolish, melanoma cell growth in this assay, consistent with MTX upregulating MITF and slowing proliferation, and TMECG being processed by low levels of TYR to inhibit DHFR. By contrast, 3D cultures were mostly free of melanoma cells after 14 days of treatment with the MTX/TMECG combination.

In an independent approach, B16/F10 melanoma cells were injected subcutaneously into C57BL/6 mice, a syngeneic melanoma model in which the host mice retain an intact immune system that plays a major role in the evolution of human melanoma (Zaidi et al., 2011). Compared to untreated mice, tumor growth was significantly reduced by TMECG treatment, but not by MTX treatment (Figures 6B and S4A). Tumors extracted from MTX-treated mice were softer, easy to dissociate, and more melanized than those obtained for vehicle-treated mice, consistent with MTX-induced expression of MITF and TYR activity. Strikingly however, the combination of MTX and TMECG acted synergistically to inhibit tumor growth.

Because tumor volume is not always a direct indication of live tumors cells (Figure S4A), we next employed a different mouse melanoma model using B16/F10 melanoma cells expressing a luciferase reporter (Figures 6C and S4B). Quantification of the in vivo luminescence signal confirmed that the MTX/TMECG combination was highly effective at reducing tumor burden. Whereas MTX or TMECG alone had an approximately 2-fold effect, a synergistic reduction in luciferase was seen using the combination (Figure S4B, left panels). Importantly, between day 6 and day 12, MTX or TMECG alone led to decreased numbers of melanoma cells in the tumors compared to vehicle-treated mice; however, by day 12 the MTX/TMECG combination had reduced the number of melanoma cells within the tumors compared to day 6, an indication of an effective therapeutic response (Figure S2B, right panel). B16/F10 tumors treated with DMSO showed their usual histological appearance of poor differentiation and limited necrosis (Figure 6D, upper panel). In contrast, 14 days treatment with MTX/TMECG induced obvious hemorrhagic necrosis, with necrotic areas of approximately 75% (Figure 6D, lower panels). Necrosis in splenic tumors was less evident when mice were treated with MTX or TMECG alone (4% ± 2%; and 11% ± 3%, respectively; data not shown). Consistent with the results obtained in cultured melanoma cells, MTX effectively induced MITF expression in mice as determined by western blotting of tumors in vivo (Figure S4C, left panel) or western blotting or immunofluorescence of dissociated tumor cells (Figures S4C, right panel, and S4D, respectively).

Significantly any residual cells surviving MTX/TMECG treatment in vivo retained their sensitivity to the drug combination. Dissociated luciferase-tagged B16/F10 tumor cells from vehicle or MTX/TMECG-treated mice were assayed for luciferase activity immediately after plating or 3 days later. Cells from both vehicle and MTX/TMECG-treated animals were able to proliferate in culture in the absence of drug, but treatment with MTX/TMECG retained its efficacy, reducing luciferase activity and cell number up to 18-fold, irrespective of whether they were derived from control or MTX/TMECG-treated mice (Figures 6E–6G). Thus, any cells in vivo surviving MTX/TMECG treatment do not appear to acquire genetic or phenotypic resistance to the drug combination.

Because elevated MITF expression in response to MTX inhibits invasiveness (Figure 1E), we next tested whether MTX/TMECG administration after injection of melanoma cells could prevent melanoma dissemination from the spleen to the liver, one of the preferential metastatic locations for melanomas. Luciferase-tagged B16/F10 cells were injected into the spleens of C57BL/6 mice, and, after 14 days treatment, tumor expansion was measured. Luciferase imaging showed that MTX/TMECG-treated mice had a substantially lower burden of macroscopic liver metastases (Figure 7A), with no mice bearing >25 macroscopic liver metastases compared with controls (Figure 7B). Histological analysis of livers (Figure 7C) revealed that when calculated as the percentage of liver volume, metastatic volume was 55% ± 12% for vehicle and 6% ± 2% for MTX/TMECG-treated

(F) E2F1 shRNAs significantly inhibit MTX/TMECG-induced apoptosis in SK-MEL-28 cells. siCN- and siE2F1-transfected cells were treated for 3 days with MTX/TMECG before apoptosis quantification. Data are presented as percent apoptosis compared to MTX/TMECG-treated siCN cells (100%) from three independent experiments. Silencing of E2F1 was verified by *WB*: lane 1, siCN; lanes 2 and 3, siE2F1 (shRNAs HSS103015 and HSS103016, respectively).
See also Figure S3 and Table S2.

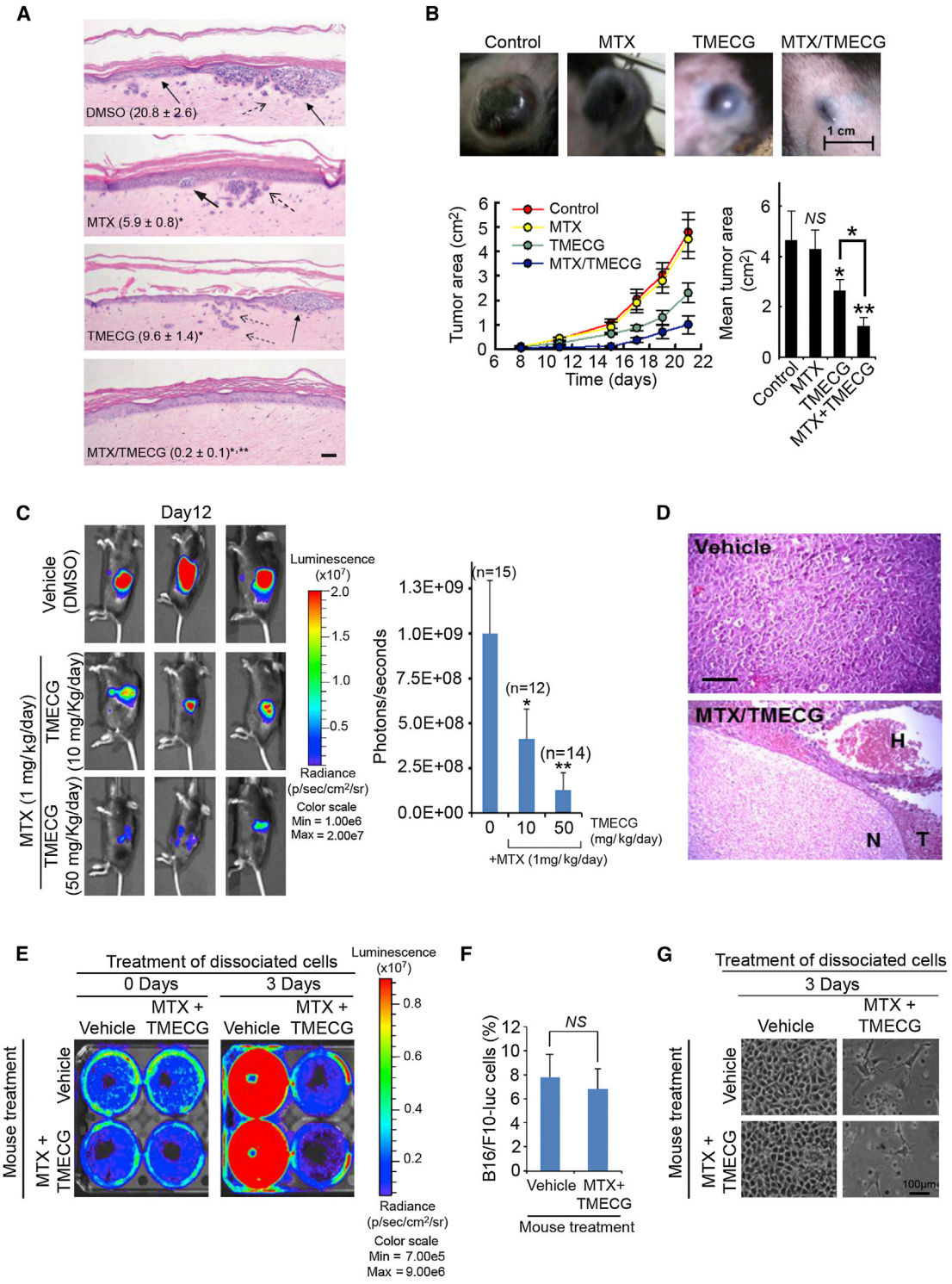

Figure 6. MTX and TMECG Combination Therapy Is Effective In Vivo

(A) A375 melanoma cells were included in a human reconstructed skin model and were treated with MTX (1 μM) and/or TMECG (10 μM) for 14 days. Medium, containing the indicated drugs was replenished every other day. The ratios of tumor versus skin areas are indicated. *$p < 0.05$ when compared with vehicle-treated skins. **$p < 0.05$ when compared with individual MTX and TMECG treatments. Scale bar = 150 μm and refers to all panels.

(B) B16/F10 melanoma cells were injected subcutaneously into C57BL/6 mice. Images show tumor size 17 days postinjection in control and treated mice. The time-dependent evolution of tumors and the mean tumor area (±SD) after 21 days of treatment are shown. *$p < 0.05$; **$p < 0.005$; NS, not statistically significant.

(C) Luciferase imaging of control and MTX/TMECG-treated mice 12 days posttumor cell injection. Firefly luciferin (120 mg/kg of mouse) was injected intraperitoneally. The values (means ± SD) are representative of three independent experiments. *$p = 0.007$; **$p = 0.002$. Results of individual treatments are described in Figure S4.

(legend continued on next page)

mice ($p = 0.002$). These data were also confirmed by real-time RT-PCR analysis designed to detect melanoma specific *TYR* mRNA in mouse livers (Figure 7D). Thus, the MTX/TMECG combination leads to a dramatic inhibition of melanoma growth both in vitro and in vivo.

Finally, we also assessed MTX/TMECG combination for potential toxicity in mice. After administration, neither MTX nor TMECG affected the levels or clearance of the other compound in plasma (Figures S5A and S5B, respectively; Table S3), and, although high doses of MTX (10 mg/kg/day) induced some weight loss in mice as expected, the doses of MTX used to treat melanoma in this study alone (1 mg/kg/day) or in combination with up to 50 mg/kg/day TMECG had no effect on mouse weight (Figure S5C). Moreover, no obvious deleterious effect of the MTX or TMECG combination was evident on nonmelanoma TYR- and MITF-positive cells such as skin melanocytes (Figure 7E) or the pigmented eye epithelia of the retina (RPE) and iris (IPE) (Figure 7F) presumably because unlike melanoma, these TYR/MITF-positive cells are not proliferating and are therefore insensitive to DHFR inhibition and dTTP depletion.

DISCUSSION

A major challenge in cancer therapy is to identify approaches that take into account resistance dictated by both irreversible genetic diversity and reversible microenvironment-driven phenotypic heterogeneity. Melanoma affords an excellent model system to explore such therapeutic options. Recent advances have identified key genetic drivers of melanoma progression and the origins of genetic resistance to targeted anti-BRAF therapy. Moreover, because MITF-negative cells are invasive, have stem-like properties, and are able to initiate tumors (Carreira et al., 2006; Cheli et al., 2011; Hoek and Goding, 2010), therapies that upregulate MITF have clear advantages.

The MTX/TMECG combination therapy used here (summarized in Figure 8) is highly effective in vitro and in vivo and has several key advantages compared to more conventional strategies. First, by upregulating MITF, MTX potentially depletes the pool of invasive melanoma cells that drive metastasis formation; second, the effectiveness of the therapy is strictly dependent on processing of the TMECG prodrug by TYR, a melanocyte-specific gene, thereby avoiding damage to other cell types, which is a major disadvantage of conventional chemotherapies; third, by inducing dTTP depletion through targeting an essential enzyme, the MTX/TMECG combination therapy is effective in melanoma cells irrespective of their *BRAF* or *MEK* status and is not susceptible to resistance arising from genetic heterogeneity within the MAPK pathway, the major cause of resistance to anti-BRAF therapies; and fourth, the proapoptotic effects of dTTP depletion in response to MTX/TMECG is independent of p53 status. Thus, the combination of MTX/TMECG overcomes many of the genetic and phenotypic heterogeneity issues that are major barriers to current antimelanoma therapy. Although we did not detect resistance among the residual population of tumor cells in MTX/TMECG-treated mice, resistance could potentially arise, for example, via genetic or epigenetic inactivation of *TYR*, *E2F1*, or *p73*. For this reason, as with any targeted therapy, it is crucial to treat patients when the tumor burden is low, because the heterogeneity that drives therapeutic resistance increases with the number of cancer cells.

Importantly, MTX is in widespread clinical use for a variety of steroid-recalcitrant inflammatory diseases, and our preliminary observations indicate that TMECG alone or in combination with MTX is not toxic in vivo, even to nonmelanoma pigment cells, and exhibits good pharmacokinetic profiles. As such, the MTX/TMECG combination therapy has potential for rapid application in a human setting.

Our observation that MTX increases *MITF* expression, and consequently the expression of multiple melanosomal components, may also partly provide an explanation for the fact that melanomas, compared to epithelial cells, are highly resistant to the effects of MTX alone. Accumulating evidence indicates that melanosomes, whose biogenesis is promoted by MITF, contribute to the refractory properties of melanoma cells by sequestering cytotoxic drugs and increasing melanosome-mediated drug export. Moreover, folate-receptor-α (FRα)-mediated endocytotic transport of MTX facilitates melanosomal drug sequestration and cellular export in melanoma cells, thereby reducing the accumulation of MTX in intracellular compartments (Sánchez-del-Campo et al., 2009b). Thus MTX-driven upregulation of MITF and consequent increased melanosome biogenesis may promote MTX resistance. In this respect, the combination of TMECG in combination with MTX used here bypasses this barrier to MTX monotherapy.

Although MTX upregulates *MITF* mRNA and protein expression, how MTX activates the *MITF* promoter is not fully understood, though preliminary results (data not shown) indicate that MTX upregulates expression of Sox10, a known regulator of *MITF* expression (Lee et al., 2000). Nevertheless, MITF is necessary for the synergy with TMECG to be achieved, but increased expression of MITF in the absence of MTX would not be sufficient; MTX plays additional roles including inducing E2F1 demethylation and depletion of DHF pools that are key components of MTX/TMECG combination therapy (see below). Moreover,

(D) Sections stained with hematoxylin and eosin (H&E) staining show the effect of MTX/TMECG on B16/F10 primary splenic tumors. Xenograft tumors treated with DMSO (vehicle) or MTX/TMECG (1 mg/kg/day and 50 mg/kg/day, respectively) over 14 days. Vehicle-treated tumors showed no discernible necrosis (N), whereas MTX/TMECG-treated tumors showed hemorrhagic (H) necrosis with obvious dividing line between viable (T) and necrotic tissues. Representative images taken from two independent experiments (n = 5 for each experiment). Scale bar = 200 μm and is applicable to both panels.

(E) B16/F10 melanoma cells, expressing a luciferase reporter, were injected subcutaneously to mice. Mice were divided in two groups (n = 7) and treated with vehicle (DMSO) or MTX/TMECG (1 mg/kg/day and 10 mg/kg/day, respectively) over 21 days. Then, tumors were pooled and dissociated. B16/F10 cells extracted from tumors were examined for their sensitivity to the MTX/TMECG combination (1 and 10 μM, respectively) using quantification of the luminescence signal (left panel).

(F) The histogram represents the number of B16/F10-*luc2* cells remaining after 3 days of MTX/TMECG treatment with respect to vehicle-treated controls (100%). Mean ± SD was calculated in triplicate (NS, not statistically significant).

(G) The morphology of tumor dissociated B16/F10-*luc2* cells before and after of MTX/TMECG treatment. Scale bar refers to all panels.

See also Figure S4.

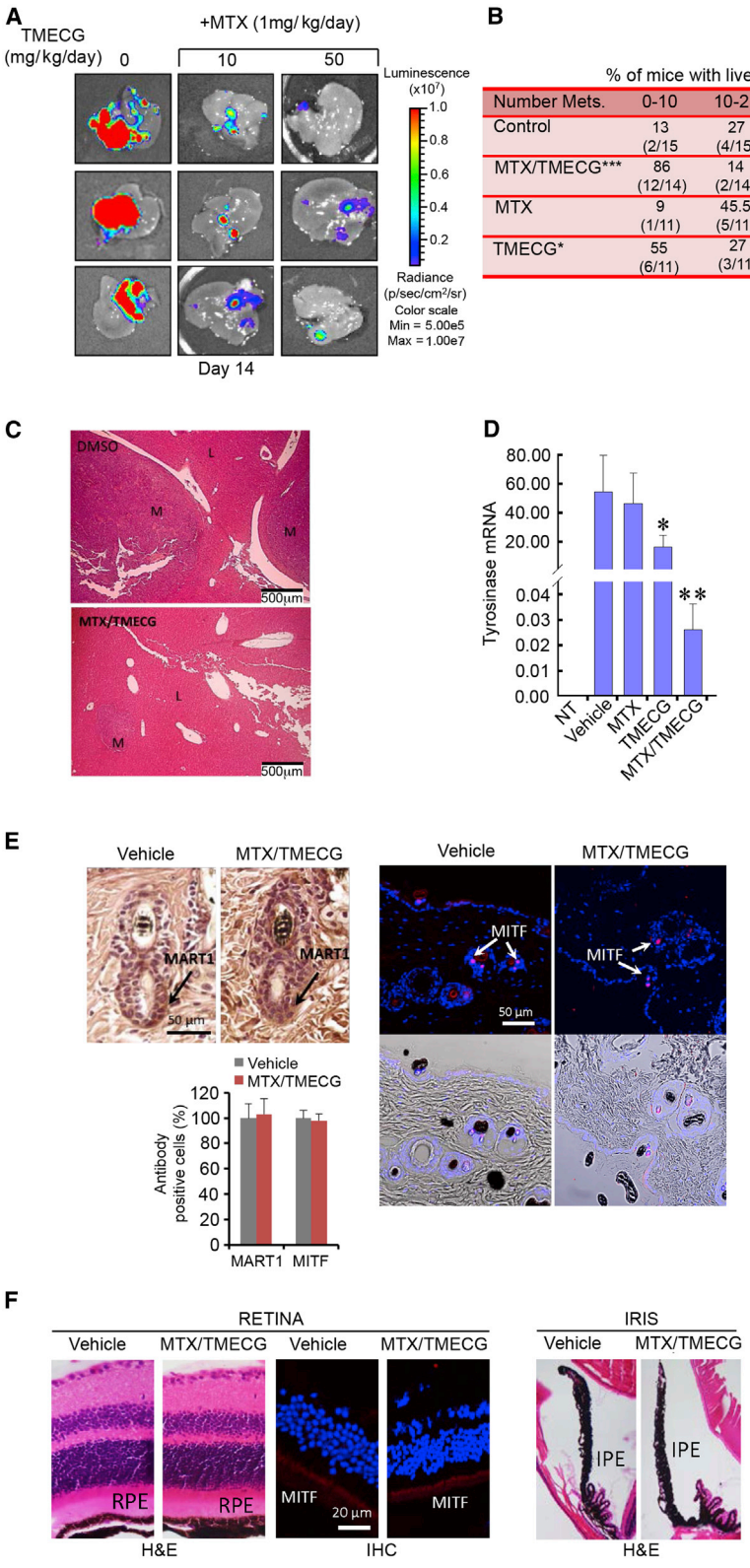

Figure 7. MTX and TMECG Combination Therapy Inhibits Metastasis and Does Not Affect Nonmelanoma Pigment Cells In Vivo

(A) Bioluminescent imaging of livers at 14 days postintrasplenic injection of B16-F10-*luc2* cells from untreated and MTX/TMECG-treated mice are shown.

(B) Quantification of macrometastases (0–10, 10–25, or >25) after treatment with vehicle (control), MTX (1 mg/kg/day), and/or TMECG (50 mg/kg/day). *Differences were statistically significant with respect to vehicle-treated mice ($p < 0.05$). **$p < 0.005$ when compared with TMECG-treated mice.

(C) H&E-stained, 4 µm formalin-fixed, paraffin-embedded liver sections from control (DMSO) and MTX/TMECG-treated mice (1 and 50 mg/kg/day, respectively).

(D) Histograms represent the number of copies of *TYR* mRNA for every 1×10^3 copies of β-actin ±SD of three independent experiments. Mice were treated with vehicle, MTX (1 mg/kg/day), and/or TMECG (50 mg/kg/day). Asterisks show statistically significant differences when compared with untreated controls (vehicle) (*$p = 0.005$; **$p = 0.001$) Livers from noninoculated mice (NT) were used as a control.

(E) Toxicological assays of the effect of MTX and/or TMECG on skin melanocyte integrity. MTX/TMECG treatment (20 days; 1 mg/kg/day and 50 mg/kg/day, respectively) did not influence number and morphology of mouse skin melanocytes. Error bars for histograms represent means ± SD.

(F) Microscopic analysis (40× magnification) H&E stain of mouse retina and retinal pigmented epithelium (RPE) and MITF immunostaining (left panel), or iridal melanocytes (IPE) (right panel), indicating no obvious differences following 20 days MTX/TMECG treatment. Scale bar refers to all panels.

See also Figure S5 and Table S3.

although both MTX and TMECG target DHFR, there is a very important difference between the two drugs. It is well known that antifolates like MTX deplete dTTP in sensitive cells; however, over several hours the endocytotic-mediated transport of MTX facilitates its cellular export, greatly reducing intracellular MTX levels in melanoma (Sánchez-del-Campo et al., 2009b). However, as we show here, MTX, before leaving the cells, modifies the posttranslational status of E2F1 leading to its activation. E2F1 activation should, therefore, allow S phase transition in cells, and importantly for melanoma survival, cells would recover an operative folate cycle (see detailed model in Figure S6). In the absence of exported MTX, high levels of thymidylate synthase and DHFR would impede the lethal depletion of dTTP and, in turn, would produce a nucleotide imbalance that would favor dTTP excess. In addition, by depleting the levels of folate receptor-alpha (FR-α), MTX also depletes cellular pools of DHF, the natural substrate of DHFR.

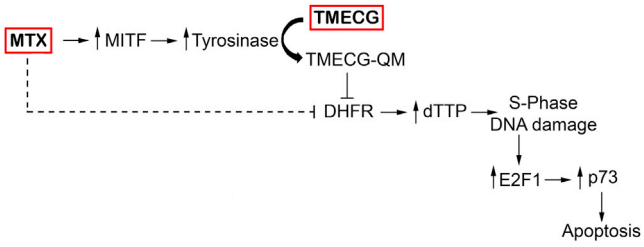

Figure 8. Summary of MTX/TMECG Therapeutic Strategy

MTX activation of *MITF* and consequently *TYR* activates the melanoma-specific antifolate activity of TMECG, leading to depletion of cellular dTTP and E2F1-mediated apoptosis. MTX therefore directs melanoma cells away from an invasive state (see Figure 1A), and targeting DHFR, an essential enzyme, in a melanoma-specific fashion induces highly efficient apoptosis in vitro and in vivo. Note that whereas activation of TYR expression is associated with differentiation, TYR-positive melanoma cells can proliferate. The dashed line represents the inhibition of DHFR by MTX at early times in the treatment. Although MTX is exported out of melanoma cells over several hours, it is likely to inhibit DHFR prior to being exported from cells.
See also Figure S6.

Because, TMECG-QM, the form of TMECG produced by TYR activity, is a competitive inhibitor of DHFR with respect to DHF, this depletion may favor the irreversible binding of TMECG-QM to its target enzyme, DHFR. Under these conditions, efficient inhibition of DHFR by TMECG-QM would lead to dTTP depletion (Figure S6). In fact, we hypothesize that because MTX induces cellular depletion of DHF in melanoma, combined therapies could efficiently inhibit DHFR if antifolates were transported into cells by an FRα-independent process, as is the case of TMECG (Sáez-Ayala et al., 2012).

The results presented here also have implications for understanding the functionality of proapoptotic pathways in melanoma. Starvation of the DNA precursor, dTTP, kills bacterial and eukaryotic cells alike. Despite numerous studies, the mechanism behind this toxicity remains unknown, although the incorporation of incorrect nucleotides and subsequent excision is the most accepted explanation. Thus, cell death induced by dTTP depletion has been associated with common pathways that regulate apoptosis. The stabilization and subsequent accumulation of the p53 tumor-suppressor has been proposed as the signal that initiates apoptosis and prevents nucleotide misincorporation during DNA synthesis and repair (Elledge et al., 1995). However, inhibitors of dTTP synthesis can cause apoptotic cell death in cells lacking a functional p53 protein, suggesting the existence of p53-independent mechanisms of "thymineless" stress-induced apoptosis (Muñoz-Pinedo et al., 2001; Myers et al., 2009; Rodriguez and Meuth, 2006; Sidi et al., 2008). More recently, it has been proposed that "thymineless" death may be mediated by the E2F1 apoptotic cascade (Wang et al., 2005). Our results strongly favor this hypothesis and are consistent with E2F1, CHK1, CHK2, and p73-mediated p53-independent cell death occurring after the dTTP depletion/DNA damage that was induced by the MTX/TMECG treatment of melanoma cells.

In conclusion, by exploiting our in-depth knowledge of the molecular mechanisms underlying phenotype switching in melanoma, we have developed a highly effective antimelanoma therapy. Importantly, this therapy is likely to be effective in patients with resistance to BRAF and MEK inhibitors and consequently may have a major impact in eradicating BRAF-resistant cells following anti-BRAF therapy.

EXPERIMENTAL PROCEDURES

Reagents and Antibodies

TMECG was synthesized from catechin (Sánchez-del-Campo et al., 2008). MTX was obtained from Sigma (Madrid, Spain). Antibodies used in this study are listed in Supplemental Experimental Procedures.

Cell Lines, Proliferation, and Apoptosis Assays

Cell lines were obtained from ATCC and maintained in the appropriate culture medium supplemented with 10% fetal bovine serum (FBS) and antibiotics. Cell viability was evaluated using the 3-(4,5-dimethylthiazol-2-yl)-2,5-diphenyltetrazolium bromide (MTT) cell proliferation assay. Apoptosis was determined using an ELISA assay (Cell Death Detection ELISAPLUS, Roche) described in more detail in Supplemental Experimental Procedures.

Tumor Dissociation

Whole subcutaneous melanoma tumors were resected en bloc, including the overlying and immediate surrounding skin and subcutaneous tissue. Tumors were then minced, mechanically disaggregated, and passed through a 100 μm filter using ice-cold RPMI1640 supplemented with 10% FBS, to achieve a single cell suspension. Live cells were counted using trypan blue and used for indicated experiments.

RNA Interference

Specific Stealth siRNAs for *MITF* (HSS142939 and HSS142940), *E2F1* [HSS103015 (siRNA1) and HSS103016 (siRNA2)], and *p53* (HSS129934 and HSS129936) were obtained from Invitrogen and transfected into melanoma cells using Lipofectamine 2000 (Invitrogen). TYR expression was knocked down using specific human siRNAs (sc-36766; Santa Cruz Biotechnology) and LipofectAMINE 2000 using standard protocols specified by the suppliers. Treatments were started 24 hr after siRNA transfection. siRNA-negative controls were used as control oligonucleotides, and the ability of the siRNA oligonucleotides to knock down the expression of the selected genes was analyzed by western blotting 24 hr after siRNA transfection.

Dinucleotide Triphosphate Pool Extraction and Analysis

Asynchronously proliferating SK-MEL-28 cells were seeded in 6-well dishes. The extraction and analysis of the dinucleotide triphosphate (dNTP) pools in each extract were carried out as described previously (Angus et al., 2002).The reaction mixtures (50 μl) contained 100 mM HEPES buffer (pH 7.5) 10 mM $MgCl_2$, 0.1 units of the *Escherichia coli* DNA polymerase I Klenow fragment (Sigma), 0.25 μM oligonucleotide template, and 1 μCi [^{3}H]dATP (ARC) or [^{3}H]dTTP (PerkinElmer). Incubation was carried out for 60 min at 37°C.

Image Acquisition, Quantification of Western Blots, and Statistical Analysis

Western blot and microscopy data have been repeated at least three times, and similar results were obtained. The results from one experiment are shown. For quantification, western blot results were scanned with a Bio-Rad Chemi-Doc scanning densitometer (Bio-Rad). For other experiments, the mean ± SD for five determinations in triplicate were calculated. Numeric data were analyzed for statistical significance using Mann-Whitney test for comparison of means with SPPS statistical software for Microsoft Windows, release 6.0 (Professional Statistic). Individual comparisons were made with Student's two-tailed, unpaired t test. The criterion for significance was $p < 0.05$ for all comparisons.

Ethical Approvals

Human tumor samples were collected from patients attending the melanoma service at Oxford University Hospital; all provided written informed consent. The protocol was approved by Oxfordshire Research Ethics Committee C (reference 09/H0606/5). All animal procedures were approved by the Ethical

Committee of the University of Murcia and the Direccion General de Ganaderia y Pesca, Comunidad Autonoma de Murcia (Project reference A1311121507).

The following experimental procedures are described in Supplemental Information: antibodies, PCR analysis, apoptosis assays, comet assay, invasion assay, ChIP assays, immunoblotting and immunoprecipitation, microscopy, MALDI-TOF mass spectroscopy, reconstituted skin, primary melanoma cells and lentivirus infection, mouse melanoma models, pharmacokinetic studies, and toxicology.

SUPPLEMENTAL INFORMATION

Supplemental Information includes Supplemental Experimental Procedures, six figures, and three tables and can be found with this article online at http://dx.doi.org/10.1016/j.ccr.2013.05.009.

ACKNOWLEDGMENTS

This work was supported by grants from Ministerio de Ciencia e Innovación (MICINN; SAF2009-12043-C02-01) and Fundación Séneca, Región de Murcia (FS-RM; 15230/PI/10) to J.N.R-L., J.C.-H., and A.P.-M., and EU ERA293514 to J.N.R.-L. J.C.-H. is contracted by the FFIS. S.C. is contracted by EU ERA293514. M.S.-A. and M.P.F.-P. have fellowships from MICINN, and L.S.-d.-C. has a fellowship from FS-RM. M.F.M. is contracted by Fundación de la Asociación Española Contra el Cáncer (FAECC). L.S.-d.-C. and C.R.G. are supported by the Ludwig Institute for Cancer Research. The authors thank Dr. Torrecillas from the Servicio de Apoyo a la Investigación (UMU) for his help in the proteomic experiments, Prof. Elisa Escudero (Department of Pharmacology, UMU) for her help with pharmacokinetic data analysis, Donata Rimoldi (Lausanne) for kindly providing the BRAF-inhibitor-resistant cell lines, and Dr. Marcelino Avilés-Trigueros (Department of Ophthalmology, UMU) for his help in retina analysis. The University of Murcia holds a patent on methods for the synthesis and therapeutic uses of TMECG and combination therapy with MTX.

Received: November 15, 2012
Revised: February 27, 2013
Accepted: May 9, 2013
Published: June 20, 2013

REFERENCES

Angus, S.P., Wheeler, L.J., Ranmal, S.A., Zhang, X., Markey, M.P., Mathews, C.K., and Knudsen, E.S. (2002). Retinoblastoma tumor suppressor targets dNTP metabolism to regulate DNA replication. J. Biol. Chem. *277*, 44376–44384.

Arnheiter, H. (2010). The discovery of the microphthalmia locus and its gene, Mitf. Pigment Cell Melanoma Res. *23*, 729–735.

Bennett, D.C. (2008). How to make a melanoma: what do we know of the primary clonal events? Pigment Cell Melanoma Res. *21*, 27–38.

Blagosklonny, M.V. (2005). Why therapeutic response may not prolong the life of a cancer patient: selection for oncogenic resistance. Cell Cycle *4*, 1693–1698.

Box, N.F., and Terzian, T. (2008). The role of p53 in pigmentation, tanning and melanoma. Pigment Cell Melanoma Res. *21*, 525–533.

Brabletz, T., Jung, A., Spaderna, S., Hlubek, F., and Kirchner, T. (2005). Opinion: migrating cancer stem cells - an integrated concept of malignant tumour progression. Nat. Rev. Cancer *5*, 744–749.

Carreira, S., Goodall, J., Aksan, I., La Rocca, S.A., Galibert, M.D., Denat, L., Larue, L., and Goding, C.R. (2005). Mitf cooperates with Rb1 and activates p21Cip1 expression to regulate cell cycle progression. Nature *433*, 764–769.

Carreira, S., Goodall, J., Denat, L., Rodriguez, M., Nuciforo, P., Hoek, K.S., Testori, A., Larue, L., and Goding, C.R. (2006). Mitf regulation of Dia1 controls melanoma proliferation and invasiveness. Genes Dev. *20*, 3426–3439.

Cheli, Y., Ohanna, M., Ballotti, R., and Bertolotto, C. (2010). Fifteen-year quest for microphthalmia-associated transcription factor target genes. Pigment Cell Melanoma Res. *23*, 27–40.

Cheli, Y., Giuliano, S., Botton, T., Rocchi, S., Hofman, V., Hofman, P., Bahadoran, P., Bertolotto, C., and Ballotti, R. (2011). Mitf is the key molecular switch between mouse or human melanoma initiating cells and their differentiated progeny. Oncogene *30*, 2307–2318.

Cheli, Y., Giuliano, S., Fenouille, N., Allegra, M., Hofman, V., Hofman, P., Bahadoran, P., Lacour, J.P., Tartare-Deckert, S., Bertolotto, C., and Ballotti, R. (2012). Hypoxia and MITF control metastatic behaviour in mouse and human melanoma cells. Oncogene *31*, 2461–2470.

Curtin, J.A., Busam, K., Pinkel, D., and Bastian, B.C. (2006). Somatic activation of KIT in distinct subtypes of melanoma. J. Clin. Oncol. *24*, 4340–4346.

Davies, H., Bignell, G.R., Cox, C., Stephens, P., Edkins, S., Clegg, S., Teague, J., Woffendin, H., Garnett, M.J., Bottomley, W., et al. (2002). Mutations of the BRAF gene in human cancer. Nature *417*, 949–954.

Dobbelstein, M., Strano, S., Roth, J., and Blandino, G. (2005). p73-induced apoptosis: a question of compartments and cooperation. Biochem. Biophys. Res. Commun. *331*, 688–693.

Du, J., Miller, A.J., Widlund, H.R., Horstmann, M.A., Ramaswamy, S., and Fisher, D.E. (2003). MLANA/MART1 and SILV/PMEL17/GP100 are transcriptionally regulated by MITF in melanocytes and melanoma. Am. J. Pathol. *163*, 333–343.

Elledge, R.M., Gray, R., Mansour, E., Yu, Y., Clark, G.M., Ravdin, P., Osborne, C.K., Gilchrist, K., Davidson, N.E., Robert, N., et al. (1995). Accumulation of p53 protein as a possible predictor of response to adjuvant combination chemotherapy with cyclophosphamide, methotrexate, fluorouracil, and prednisone for breast cancer. J. Natl. Cancer Inst. *87*, 1254–1256.

Fedorenko, I.V., Paraiso, K.H., and Smalley, K.S. (2011). Acquired and intrinsic BRAF inhibitor resistance in BRAF V600E mutant melanoma. Biochem. Pharmacol. *82*, 201–209.

Fidler, I.J. (1978). Tumor heterogeneity and the biology of cancer invasion and metastasis. Cancer Res. *38*, 2651–2660.

Garraway, L.A., Widlund, H.R., Rubin, M.A., Getz, G., Berger, A.J., Ramaswamy, S., Beroukhim, R., Milner, D.A., Granter, S.R., Du, J., et al. (2005). Integrative genomic analyses identify MITF as a lineage survival oncogene amplified in malignant melanoma. Nature *436*, 117–122.

Goodall, J., Carreira, S., Denat, L., Kobi, D., Davidson, I., Nuciforo, P., Sturm, R.A., Larue, L., and Goding, C.R. (2008). Brn-2 represses microphthalmia-associated transcription factor expression and marks a distinct subpopulation of microphthalmia-associated transcription factor-negative melanoma cells. Cancer Res. *68*, 7788–7794.

Hallstrom, T.C., Mori, S., and Nevins, J.R. (2008). An E2F1-dependent gene expression program that determines the balance between proliferation and cell death. Cancer Cell *13*, 11–22.

Hodgkinson, C.A., Moore, K.J., Nakayama, A., Steingrímsson, E., Copeland, N.G., Jenkins, N.A., and Arnheiter, H. (1993). Mutations at the mouse *microphthalmia* locus are associated with defects in a gene encoding a novel basic-helix-loop-helix-zipper protein. Cell *74*, 395–404.

Hoek, K.S., and Goding, C.R. (2010). Cancer stem cells versus phenotype-switching in melanoma. Pigment Cell Melanoma Res. *23*, 746–759.

Kinner, A., Wu, W., Staudt, C., and Iliakis, G. (2008). Gamma-H2AX in recognition and signaling of DNA double-strand breaks in the context of chromatin. Nucleic Acids Res. *36*, 5678–5694.

Kobi, D., Steunou, A.L., Dembélé, D., Legras, S., Larue, L., Nieto, L., and Davidson, I. (2010). Genome-wide analysis of POU3F2/BRN2 promoter occupancy in human melanoma cells reveals Kitl as a novel regulated target gene. Pigment Cell Melanoma Res. *23*, 404–418.

Kontaki, H., and Talianidis, I. (2010). Lysine methylation regulates E2F1-induced cell death. Mol. Cell *39*, 152–160.

Lee, M., Goodall, J., Verastegui, C., Ballotti, R., and Goding, C.R. (2000). Direct regulation of the Microphthalmia promoter by Sox10 links Waardenburg-Shah syndrome (WS4)-associated hypopigmentation and deafness to WS2. J. Biol. Chem. *275*, 37978–37983.

Lin, W.C., Lin, F.T., and Nevins, J.R. (2001). Selective induction of E2F1 in response to DNA damage, mediated by ATM-dependent phosphorylation. Genes Dev. *15*, 1833–1844.

Loercher, A.E., Tank, E.M., Delston, R.B., and Harbour, J.W. (2005). MITF links differentiation with cell cycle arrest in melanocytes by transcriptional activation of INK4A. J. Cell Biol. *168*, 35–40.

Lopez-Bergami, P. (2011). The role of mitogen- and stress-activated protein kinase pathways in melanoma. Pigment Cell Melanoma Res. *24*, 902–921.

Martínez-Balbás, M.A., Bauer, U.M., Nielsen, S.J., Brehm, A., and Kouzarides, T. (2000). Regulation of E2F1 activity by acetylation. EMBO J. *19*, 662–671.

Muñoz-Pinedo, C., Oliver, F.J., and López-Rivas, A. (2001). Apoptosis of haematopoietic cells upon thymidylate synthase inhibition is independent of p53 accumulation and CD95-CD95 ligand interaction. Biochem. J. *353*, 101–108.

Myers, K., Gagou, M.E., Zuazua-Villar, P., Rodriguez, R., and Meuth, M. (2009). ATR and Chk1 suppress a caspase-3-dependent apoptotic response following DNA replication stress. PLoS Genet. *5*, e1000324.

Nazarian, R., Shi, H., Wang, Q., Kong, X., Koya, R.C., Lee, H., Chen, Z., Lee, M.K., Attar, N., Sazegar, H., et al. (2010). Melanomas acquire resistance to B-RAF(V600E) inhibition by RTK or N-RAS upregulation. Nature *468*, 973–977.

Nikolaev, S.I., Rimoldi, D., Iseli, C., Valsesia, A., Robyr, D., Gehrig, C., Harshman, K., Guipponi, M., Bukach, O., Zoete, V., et al. (2012). Exome sequencing identifies recurrent somatic MAP2K1 and MAP2K2 mutations in melanoma. Nat. Genet. *44*, 133–139.

Pardee, A.B., Li, C.J., and Reddy, G.P. (2004). Regulation in S phase by E2F. Cell Cycle *3*, 1091–1094.

Pinner, S., Jordan, P., Sharrock, K., Bazley, L., Collinson, L., Marais, R., Bonvin, E., Goding, C., and Sahai, E. (2009). Intravital imaging reveals transient changes in pigment production and Brn2 expression during metastatic melanoma dissemination. Cancer Res. *69*, 7969–7977.

Rodriguez, R., and Meuth, M. (2006). Chk1 and p21 cooperate to prevent apoptosis during DNA replication fork stress. Mol. Biol. Cell *17*, 402–412.

Sáez-Ayala, M., Fernández-Pérez, M.P., Montenegro, M.F., Sánchez-del-Campo, L., Chazarra, S., Piñero-Madrona, A., Cabezas-Herrera, J., and Rodríguez-López, J.N. (2012). Melanoma coordinates general and cell-specific mechanisms to promote methotrexate resistance. Exp. Cell Res. *318*, 1146–1159.

Sánchez-del-Campo, L., Otón, F., Tárraga, A., Cabezas-Herrera, J., Chazarra, S., and Rodríguez-López, J.N. (2008). Synthesis and biological activity of a 3,4,5-trimethoxybenzoyl ester analogue of epicatechin-3-gallate. J. Med. Chem. *51*, 2018–2026.

Sánchez-del-Campo, L., Tárraga, A., Montenegro, M.F., Cabezas-Herrera, J., and Rodríguez-López, J.N. (2009a). Melanoma activation of 3-*o*-(3,4,5-trimethoxybenzoyl)-(-)-epicatechin to a potent irreversible inhibitor of dihydrofolate reductase. Mol. Pharm. *6*, 883–894.

Sánchez-del-Campo, L., Montenegro, M.F., Cabezas-Herrera, J., and Rodríguez-López, J.N. (2009b). The critical role of alpha-folate receptor in the resistance of melanoma to methotrexate. Pigment Cell Melanoma Res. *22*, 588–600.

Serafino, A., Sinibaldi-Vallebona, P., Lazzarino, G., Tavazzi, B., Rasi, G., Pierimarchi, P., Andreola, F., Moroni, G., Galvano, G., Galvano, F., and Garaci, E. (2004). Differentiation of human melanoma cells induced by cyanidin-3-O-beta-glucopyranoside. FASEB J. *18*, 1940–1942.

Sidi, S., Sanda, T., Kennedy, R.D., Hagen, A.T., Jette, C.A., Hoffmans, R., Pascual, J., Imamura, S., Kishi, S., Amatruda, J.F., et al. (2008). Chk1 suppresses a caspase-2 apoptotic response to DNA damage that bypasses p53, Bcl-2, and caspase-3. Cell *133*, 864–877.

Smalley, K.S., and Flaherty, K.T. (2009). Integrating BRAF/MEK inhibitors into combination therapy for melanoma. Br. J. Cancer *100*, 431–435.

Sosman, J.A., Kim, K.B., Schuchter, L., Gonzalez, R., Pavlick, A.C., Weber, J.S., McArthur, G.A., Hutson, T.E., Moschos, S.J., Flaherty, K.T., et al. (2012). Survival in BRAF V600-mutant advanced melanoma treated with vemurafenib. N. Engl. J. Med. *366*, 707–714.

Strub, T., Giuliano, S., Ye, T., Bonet, C., Keime, C., Kobi, D., Le Gras, S., Cormont, M., Ballotti, R., Bertolotto, C., and Davidson, I. (2011). Essential role of microphthalmia transcription factor for DNA replication, mitosis and genomic stability in melanoma. Oncogene *30*, 2319–2332.

Tachibana, M., Takeda, K., Nobukuni, Y., Urabe, K., Long, J.E., Meyers, K.A., Aaronson, S.A., and Miki, T. (1996). Ectopic expression of MITF, a gene for Waardenburg syndrome type 2, converts fibroblasts to cells with melanocyte characteristics. Nat. Genet. *14*, 50–54.

Urist, M., Tanaka, T., Poyurovsky, M.V., and Prives, C. (2004). p73 induction after DNA damage is regulated by checkpoint kinases Chk1 and Chk2. Genes Dev. *18*, 3041–3054.

van Elsas, A., Zerp, S., van der Flier, S., Krüse-Wolters, M., Vacca, A., Ruiter, D.J., and Schrier, P. (1995). Analysis of N-ras mutations in human cutaneous melanoma: tumor heterogeneity detected by polymerase chain reaction/single-stranded conformation polymorphism analysis. Recent Results Cancer Res. *139*, 57–67.

Van Raamsdonk, C.D., Bezrookove, V., Green, G., Bauer, J., Gaugler, L., O'Brien, J.M., Simpson, E.M., Barsh, G.S., and Bastian, B.C. (2009). Frequent somatic mutations of GNAQ in uveal melanoma and blue naevi. Nature *457*, 599–602.

Villanueva, J., Vultur, A., and Herlyn, M. (2011). Resistance to BRAF inhibitors: unraveling mechanisms and future treatment options. Cancer Res. *71*, 7137–7140.

Visvader, J.E., and Lindeman, G.J. (2008). Cancer stem cells in solid tumours: accumulating evidence and unresolved questions. Nat. Rev. Cancer *8*, 755–768.

Wang, A., Li, C.J., Reddy, P.V., and Pardee, A.B. (2005). Cancer chemotherapy by deoxynucleotide depletion and E2F-1 elevation. Cancer Res. *65*, 7809–7814.

Zaidi, M.R., Davis, S., Noonan, F.P., Graff-Cherry, C., Hawley, T.S., Walker, R.L., Feigenbaum, L., Fuchs, E., Lyakh, L., Young, H.A., et al. (2011). Interferon-γ links ultraviolet radiation to melanomagenesis in mice. Nature *469*, 548–553.